$\Pi(Z)$ = function in Equation (21), Part II
$\rho(Z)$ = function in Equation (21), Part II
σ_k = sign of k^{th} determinant in Equation (82), Part I
$\psi(s)$ = characteristic polynomial of A

Manuscript received September 15, 1975; revision received and accepted November 25, 1975.

Part II. The Approximation Problem

The composite algorithm derived in Part I is used to construct models from pulse responses of lumped and distributed systems, as well as an empirically measured residence time density. Along the way, salient points in the numerical implementation of the algorithm are indicated. In the present recursive procedure, the initial transient is predicted accurately by lower-order partial realizations; successive partial realizations involve progressively longer tails of the pulse response. The zeroth moment of the impulse response is used to advantage when realizations with no zeros are appropriate

SCOPE

In Part I of this two-part series, a sequential algorithm was derived for obtaining practical realizations from realistic response data of continuous time systems with intermittent measurements. In Part II, the modeling procedure will be illustrated with impulse responses from numerical examples of lumped and distributed systems, as well as an empirically measured residence time density.

The question that arises in evaluating these models is: In what sense is the input/output relation of a partial realization an approximation to the given input/output relation? The answer depends on the data set used to derive these realizations. In earlier work, the moments of the impulse response have been used to derive realizations. This is possible, since the moments form a set of parameters related to powers of A^{-1} in the same way that the Markov parameters are related to powers of A in the realization (A, b, c) (Bruni, 1969). If moments are used in the realization algorithm, a low frequency approximation is obtained which may not bring out the initial transient of the original response. The Markov parameters yield a high frequency approximation which may not bring out the long time behavior of the system. Rossen (1972) has used a combined set of parameters with some moments preceding the Markov parameters to obtain in some cases a better long-time approximation. However, for other cases, he obtained unstable models for stable physical processes. The regularization procedure presented in Part I, and used here, is based on the use of Markov parameters alone. Here, we shall compare partial realizations of different dimensions in terms of their impulse responses. In this comparison, the different data sets are finite sequences of Markov parameters of increasing length. In addition, we shall discuss the range of modes that may be identified from a given impulse response.

CONCLUSIONS AND SIGNIFICANCE

The present recursive realization algorithm identifies the faster modes first and then identifies the slower modes; that is, the initial transient is predicted accurately by lower-order partial realizations; successive partial realizations have progressively longer tails. Hence, the tail of the response, if inordinately long and inaccurate, may be ignored while lower-order partial realizations are constructed. This feature is a definite improvement over the method of moments, which is extremely sensitive to the tail of the response.

A distributed system may be modeled by a finite dimensional realization coupled with a time delay. The number of zero Markov parameters estimated then depends on the time delay chosen; in selecting this combination, we seek to ensure a minimal degree of smoothness in the predicted response, keeping the dimension of the realization low (at most 5).

The intensity function provides useful information for both lumped and distributed systems. As illustrated by the examples, systems with monotone increasing intensity functions are easier to model, partly because the zeroth moment can then be taken into account. When the zeroth moment is used, the value of the first nonzero Markov parameter assumes increased importance.

CHARACTERIZING THE APPROXIMATION

Sequential model building methods such as the dominant pole technique and the present recursive realization procedure may be compared with respect to the order of identification of the system's response modes. In the dominant pole technique, the slowest mode or the largest time constant is identified first; then this is peeled off from the response curve to identify the next slower mode, and so on (Sheppard, 1962, Chapter 11). In the recursive realization procedure, however, as the dimension of the partial realization increases, slower modes are added on. The impulse responses of higher-order partial realizations have progressively longer tails. This is illustrated by the partial realizations of the impulse response function (see example 4 of Part I):

$$g(t) = \frac{1}{16}(e^{-t} + e^{-3t} + 3e^{-5t} - 5e^{-7t}) \qquad (1)$$

with transfer function

$$G(s) = \frac{(s+2)(s+4)}{(s+7)(s+5)(s+3)(s+1)} \qquad (2)$$

The complete realization matrices, obtained from the first nine Markov parameters, are:

$$A = \begin{bmatrix} -10 & 1 & 0 & 0 \\ -18 & 0 & 1 & 0 \\ 12 & 0 & -2.75 & 1 \\ 0 & 0 & 0.9375 & -3.25 \end{bmatrix}; \quad b = \begin{bmatrix} 0 \\ 1 \\ 0 \\ 0 \end{bmatrix}; \quad c = [1 \quad 0 \quad 0 \quad 0] \qquad (3)$$

The unit pulse responses of the partial realizations of dimensions 2 and 3 have been compared with the unit pulse response of the complete realization in Figure 1. The settling times of these responses follow a progression from 2.5 units of time for the partial realization of dimension 2, to 4.5 units for that of dimension 3, and 5 units for the complete realization of dimension 4. The areas under these curves do not follow any such progression. The partial realizations are given by the leading principal submatrices of the complete realization matrices:

$$A_1 = \begin{bmatrix} -10 & 1 \\ -18 & 0 \end{bmatrix}; \quad b_1 = \begin{bmatrix} 0 \\ 1 \end{bmatrix}; \quad c_1 = [1 \quad 0] \quad (4)$$

$$A_2 = \begin{bmatrix} -10 & 1 & 0 \\ -18 & 0 & 1 \\ 12 & 0 & -2.75 \end{bmatrix}; \quad b_2 = \begin{bmatrix} 0 \\ 1 \\ 0 \end{bmatrix}; \quad c_2 = [1 \quad 0 \quad 0] \quad (5)$$

The eigenvalues of A_1 are -7.65 and -2.35; those of A_2 are -7.05, -4.52, and -1.176, and those of A (the complete realization) are -7, -5, -3, and -1. In terms of magnitudes, the smallest eigenvalue of A is lower than that of A_2, which in turn is lower than that of A_1. It must be pointed out here that the occurrence of real eigenvalues in all the partial realizations for this example is fortuitous. The poles of the complete realization alone have been assumed to be real. However, partial realizations, which are leading principal submatrices of the complete realization matrices, may have complex poles.

The number of modes that can be identified sequentially is limited in either technique—the dominant pole technique and the recursive realization procedure. A practical limit on the dimension of the partial realization that can be identified from response curves is 5, corresponding to ten Markov parameters. The recognition problem, centered on the number of components that can be identified in time series data, has been treated by Bergner et al. (1973). More components can be identified when there are no zeros in the system, since this situation requires the minimum number of parameters for a model of given dimension.

The smaller an eigenvalue in relation to the largest eigenvalue, the less identifiable it is since the relative contribution of the smaller eigenvalues to later Markov parameters is progressively smaller. This may be seen by noting that the impulse response may be written as

$$g(t) = \sum_{i=1}^{n} A_i e^{-\gamma_i t} \quad (6)$$

(where $\gamma_i > 0$ and A_i are real for all i) and that the Markov parameters are given by

$$Y_k = g^{(k)}(0) = \sum_{i=1}^{n} A_i(-\gamma_i)^k \quad (7)$$

For the same reason, the bulk of the value of later Markov parameters comes from the extension sequence generated from earlier parameters. From (7) it may be seen also that the stiffer the system (that is, the larger the spread among the eigenvalues), the larger the growth rate of Markov parameters, but the actual values of later Markov parameters for a stiff system will be very close to the values in the extension sequence generated from earlier Markov parameters. It is important to note that a choice of time scale is implicit in the above discussion. Once a time scale is chosen, only the modes represented by eigenvalues ranging, roughly, from $O(10)$ to $O(1)$ on that scale may be identified reliably.

MODELS FOR LUMPED SYSTEMS

We shall now present two illustrations of the modeling procedure for lumped systems. Complete details of the estimation may be found in Jayaraman (1975). The original responses are obtained from a third-order system with no zeros (example 2 of Part I) and a fourth-order system with two zeros (example 4 of Part I).

Let us consider the impulse response function of a third-order system with no zeros, given by

$$g(t) = \frac{4}{3} e^{-t/2} - 2e^{-t} + \frac{2}{3} e^{-2t} \quad (8)$$

with

$$G(s) = 1/(s^3 + 3.5s^2 + 3.5s + 1) \quad (9)$$

By using twenty-five data points with a spacing on the time axis of 0.5 units, an acceptable value is obtained for the ratio of the first two nonzero Markov parameters with two zero Markov parameters. At this point, the values obtained for the Markov parameters are

$$0, \ 0, \ 1, \ -3.5, \ 8.41, \ -15.88, \ \ldots \quad (10)$$

If we now insert $Y_0 = Y_1 = 0$ and $Y_2 = 1$, $Y_3 = -3.5$ in the factorization equation [see Equation (93) of Part I], we obtain the inequality

$$Y_4 < 12.25 \quad (11)$$

The present estimate of Y_4 satisfies this bound. We may now insert $Y_4 = 8.41$ in the factorization equation to obtain the inequalities

$$-29.5 < Y_5 < -16 \quad (12)$$

Since the present estimate of Y_5 does not satisfy the upper bound, we must go to the next stage of regression to obtain a value of Y_5 within the bounds. The result is still unsatisfactory. The reason for this difficulty may be discerned from Figure 2 which depicts the given impulse response $g(t)$ and the values fitted at each stage of regression. $g_k(t)$ is a constraint function of degree k, incorporating previously estimated, acceptable values of $(k+1)$ Markov parameters. The functions at the fourth and sixth stages have been plotted with reversed signs. From the flatness of the plot of $-(g - g_4)/t^5$, we note that at this stage, identifiability is low, indicating the presence of a small exponential. This prompts us to settle for the lowest-order partial realization, which must be of dimension three. This third-order model must have a transfer function of the form $1/(s^3 + \alpha_1 s^2 + \alpha_2 s + \alpha_3)$. The intensity function derived from the given response being monotone increasing further strengthens our belief that such a model will be adequate. However, we need six Markov parameters to construct a third-order model, so Y_5 must be estimated. Let us look at the factorization equation (at this stage we do not know the entries in parentheses):

$$\begin{bmatrix} 0 & 0 & 1 & -3.5 \\ 0 & 1 & -3.5 & 8.41 \\ 1 & -3.5 & 8.41 & (-17) \\ -3.5 & 8.41 & (-17) & (30.9) \end{bmatrix} = \begin{bmatrix} 1 & & & \\ -3.5 & 1 & & \\ 8.41 & -3.5 & 1 & \\ (-17) & 8.41 & -3.5 & 1 \end{bmatrix} \begin{bmatrix} 0 & 0 & 1 & -3.5 \\ 0 & 1 & 0 & -3.84 \\ 1 & 0 & 0 & (-1) \\ 0 & 0 & 0 & (0) \end{bmatrix} \quad (13)$$

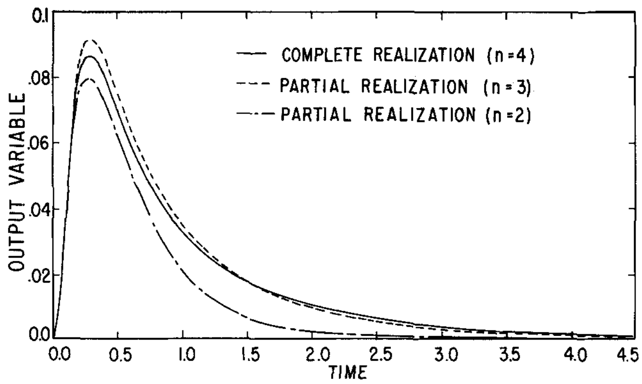

Fig. 1. Pulse responses from partial realizations of Eq. (1).

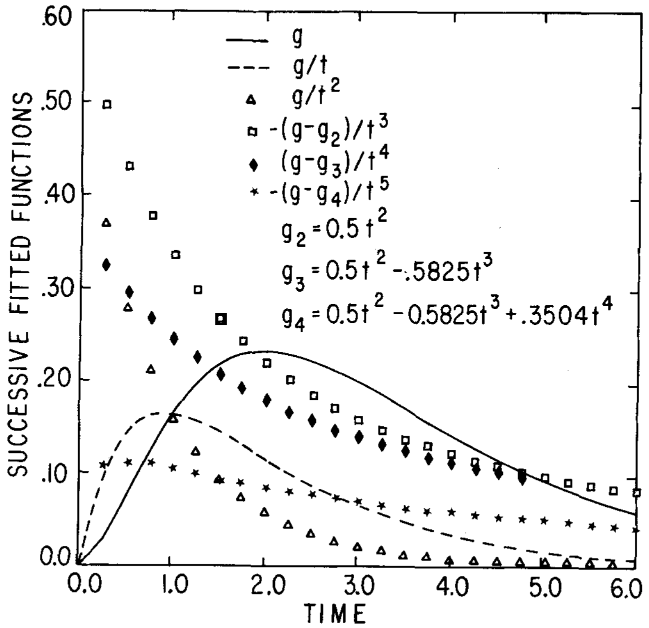

Fig. 2. Residuals in estimation of Markov parameters from time series data (data generated from Eq. (8)).

In Part I we noted that for a realization with no zeros, as in this case, A is in companion form, and hence the column immediately following the antidiagonal submatrix in Q consists of the coefficients of the characteristic polynomial of A [see Equation (6) of Part I]. The zeroth moment of the impulse response is given by $1/\alpha_3$. But this is the same as the area under the response curve, which is 1. So if we settle for a third-order model, $q_{34} = -\alpha_3 = -1$. This implies that $Y_5 = -17$. Thus the realization obtained is

$$A = \begin{bmatrix} -3.5 & 1 & 0 \\ -3.84 & 0 & 1 \\ -1 & 0 & 0 \end{bmatrix}; \quad b = \begin{bmatrix} 0 \\ 0 \\ 1 \end{bmatrix}; \quad c = [1 \quad 0 \quad 0] \tag{14}$$

This approximate realization may be compared with the exact realization in (84) of Part I. The unit pulse responses of both have been plotted in Figure 3. By taking the zeroth moment into account in identifying the model, we have been able to match the long-term behavior more closely than otherwise. Whenever we choose to model a system by a realization with no zeros, the zeroth moment can be taken into account in the same way.

We now turn to the impulse response function of a fourth-order system with two zeros, specified in Equation (1). The settling time for the response is about five units, and no scaling is necessary. Twenty data points are used with a spacing of 0.25 units on the time axis. Here, one zero Markov parameter is enough to obtain an acceptable value for the ratio of the first two nonzero Markov parameters. At this point, the values obtained for the Markov parameters are

$$0,\ 1,\ -10,\ 77.65,\ -498,\ 2\,555,\ \ldots \tag{15}$$

The dimension of the lowest-order partial realization is two. Further, the intensity function for this example is nonmonotone; it has a maximum. So the model must have some zeros, and its dimension must be greater than two. Let us now write the factorization equation with the first three Markov parameters:

$$\begin{bmatrix} 0 & 1 & -10 & Y_3 \\ 1 & -10 & Y_3 & Y_4 \\ -10 & Y_3 & Y_4 & Y_5 \\ Y_3 & Y_4 & Y_5 & \end{bmatrix} = \begin{bmatrix} 1 & & & \\ -10 & 1 & & \\ Y_3 & -10 & 1 & \\ Y_4 & Y_3 & (\ ) & 1 \end{bmatrix} \begin{bmatrix} 0 & 1 & -10 & Y_3 \\ 1 & 0 & & \\ 0 & 0 & & \\ 0 & 0 & & \end{bmatrix} \tag{16}$$

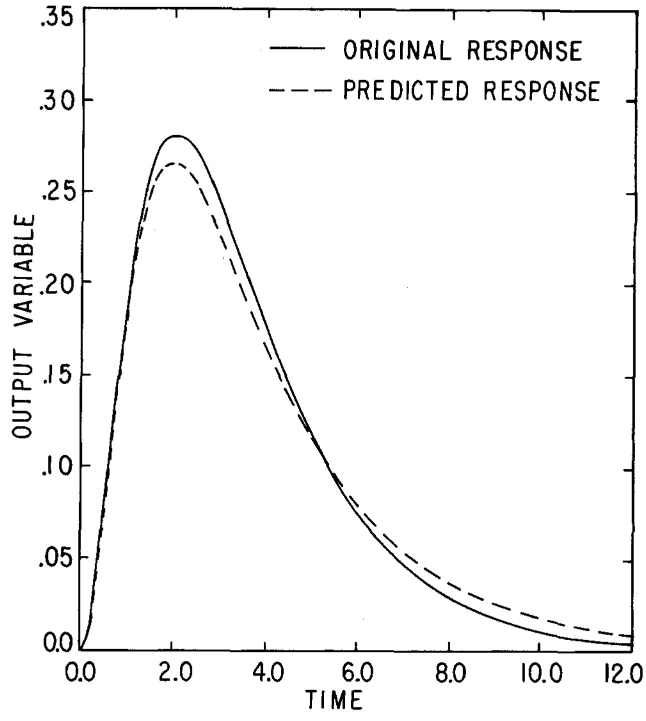

Fig. 3. Pulse response for example 2 of Part I.

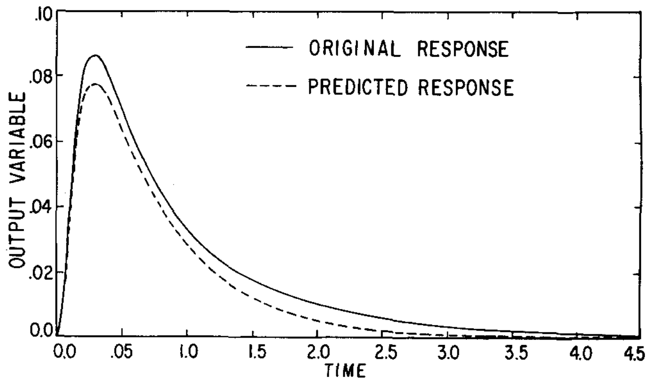

Fig. 4. Pulse response for example 4 of Part I.

According to the sign pattern described in Part I for such impulse response functions representing series parallel networks of CSTR's

$$q_{23} < 0, \text{ which implies that } Y_3 < 100 \qquad (17)$$

The sign of q_{33} cannot be prescribed. Hence, although the present value of Y_3 satisfies the bound in (17), Y_3 and Y_4 must be estimated carefully in another fit. The next stage of regression yields the following set of Markov parameters:

$$0,\ 1,\ -10,\ 81.8,\ -597,\ 3\,664,\ \ldots \qquad (18)$$

Now (16) may be rewritten as

$$\begin{bmatrix} 0 & 1 & -10 & 81.8 \\ 1 & -10 & 81.8 & -597 \\ -10 & 81.8 & -597 & 3\,664 \\ 81.8 & -597 & 3\,664 & \end{bmatrix} = \begin{bmatrix} 1 & & & \\ -10 & 1 & & \\ 81.8 & -10 & 1 & \\ -597 & 81.8 & -20.95 & 1 \end{bmatrix} \begin{bmatrix} 0 & 1 & -10 & 81.8 \\ 1 & 0 & -18.2 & 221 \\ 0 & 0 & 39 & -817 \\ 0 & 0 & 0 & \end{bmatrix} \qquad (19)$$

The revised estimate of Y_3 also satisfies the bound in (17). Since $q_{33} > 0$, we must have $q_{34} < 0$, which implies that $Y_5 < 4\,481$. The value obtained for Y_5 satisfies this bound. The resulting partial realization of dimension three is

$$A = \begin{bmatrix} -10 & 1 & 0 \\ -18.2 & 0 & 1 \\ 39 & 0 & -10.95 \end{bmatrix}; \quad b = \begin{bmatrix} 0 \\ 1 \\ 0 \end{bmatrix}; \quad c = [1 \quad 0 \quad 0] \qquad (20)$$

The unit pulse responses of this approximate realization and of the exact realization [Equation (3)] are compared in Figure 4. Till $t = 1$, the predicted response is within 5% of the original response. After $t = 1$, the tail of the predicted response is steeper than that of the original response. This indicates the presence of a slower mode in the original response than the ones identified. With a certain amount of iteration, a model of one higher dimension, 4, could be constructed to predict the tail more accurately. An extension sequence of Markov parameters may be derived from (19), giving

$$Y_6 = -13\,641 \qquad Y_7 = 86\,429$$

In accordance with the prescribed sign pattern

$$q_{44} \geq 0 \rightarrow Y_6 \geq -13\,641$$

$$q_{45} \leq 0 \rightarrow Y_7 \leq 86\,429$$

Iteration* is required here because the relative contribution of the small eigenvalues to the later Markov parameters is small.

It must be noted here that the sign patterns derived in Part I are only necessary for the complete realization to have real and negative poles. The actual approximate realizations obtained by the composite algorithm may, and frequently will, have some complex poles with negative real parts. This may be due to either, or both, of two reasons: the model identified may be of inadequate dimension, and slight errors in the coefficients of the characteristic polynomial of A can introduce complex poles in the system (Wilkinson, 1965 Chapter 7). The present identification scheme amounts to calculating the coefficients of the characteristic polynomial of A, since these constitute the last row of R^{-1} [see Part I, Equation (25)]. Nevertheless, the sign patterns derived in Part I are vital in regularizing the identification problem.

REALIZATIONS WITH TIME DELAYS FOR DISTRIBUTED SYSTEMS

We shall now describe the representation of distributed systems by linear, finite dimensional, time invariant realizations, coupled with time delays. Here again, we shall start from impulse response curves. These are obtained either from solutions of distributed models (parabolic partial differential equations) or from input/output experiments on a physical system such as a packed bed. Let us recall that the number of zero Markov parameters specifies the minimum order of precursors of rational type, defined as the smallest integer q such that $\lim s^q G(s) \neq 0$. For distributed systems, precursors will be of irrational type; following common practice, we shall restrict ourselves to precursors of rational type with delay. It must be noted that then the choice of the time delay θ and the choice of the number of zero Markov parameters q are interdependent. Once this combination is specified, the realization procedure for distributed systems follows that for lumped systems. Once again, in selecting this combination, we seek to ensure a minimal degree of smoothness in the predicted response, keeping the dimension of the resulting model low (at most 5). The requirement of smoothness cannot be met if the delay chosen is very large. On the other hand, if the delay chosen is very small, the number of zero Markov parameters estimated will be excessively large, resulting in an excessively large dimension for the lowest-order partial realization possible. This will, in turn, require a large number of nonzero Markov parameters which may not be reliably identifiable. Naturally, the time delay chosen would be near the breakthrough time for the input pulse at the output of the distributed system.

The most common distributed models in chemical engineering are one-dimensional, parabolic, partial differential equations. In modeling these by finite dimensional realizations, with time delays, the intensity function again provides a useful guideline. Karlin and MacGregor (1960) have shown that for a system represented by the equation

$$\frac{\partial u}{\partial t} = Lu \equiv \frac{1}{\rho(Z)} \frac{\partial}{\partial Z} \left[\Pi(Z) \frac{\partial u}{\partial Z} \right] \qquad (21)$$

with $\rho(Z)$ and $\Pi(Z)$ positive on the domain $(0, \infty)$ and homogeneous boundary conditions, the impulse response, which is the same as the Green's function at a fixed value of Z, is a Polya density function (Part I). This implies that the corresponding intensity function is monotone increasing (Karlin, 1968, p. 152). An equation of the form of (21) may be written for single phase transport or for two phase transport with a linear equilibrium relation between the concentrations in the two phases. Such systems may thus be modeled by a finite dimensional realization with no zeros, coupled with a time delay. However, when the operator L is replaced by an operator L_1 including a term linear in u

$$\frac{\partial u}{\partial t} = L_1 u \equiv \frac{1}{\rho(Z)} \frac{\partial}{\partial Z} \left[\Pi(Z) \frac{\partial u}{\partial Z} \right] + ku \qquad (22)$$

the resulting Green's function need not be a Polya density function; hence the corresponding intensity function may be nonmonotone. An equation of the form of (22) may be written for a two phase transport system with a finite exchange rate between the two phases. Such a model has in fact been proposed for the liquid phase in trickle flow

* On the IBM 360/91, the computer time required for a typical least-squares fit run is 0.5 s; for a realization run, it is 0.1 to 0.2 s.

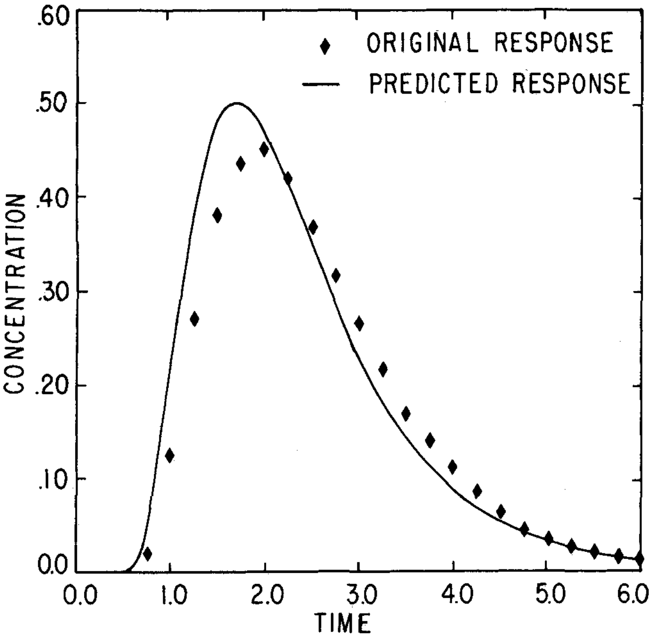

Fig. 5. Pulse response for chromatographic column with axial dispersion.

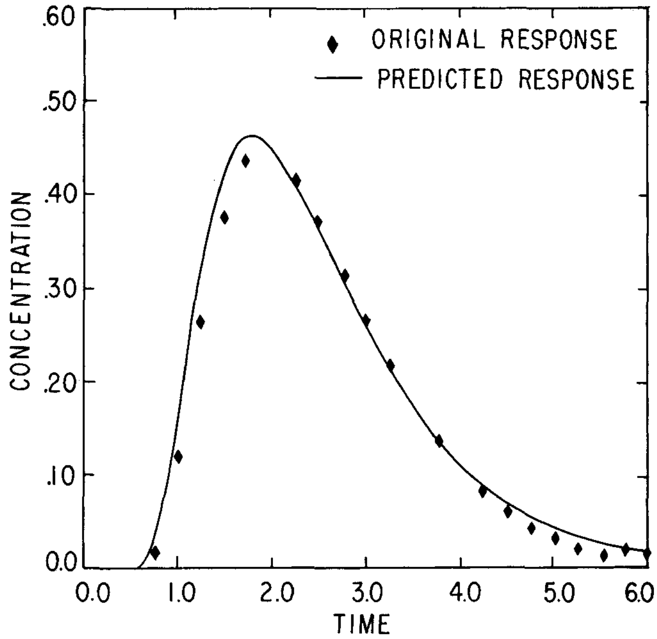

Fig. 6. Pulse response for chromatographic column with axial dispersion. Modified fourth order realization.

through a packed bed with porous packing by Bennett and Goodridge (1970). The input/output experiments performed on this kind of physical system by a number of investigators (Lapidus, 1957; Schiesser, 1959; Hoogendorn and Lips, 1965; van Swaiij, 1969) yielded residence time density functions with nonmonotone intensity functions. Finite dimensional realizations used to model such systems must have some zeros in order to bring out the latter portion of the response.

Two illustrations of models for distributed systems are presented below. Once again, details may be found in Jayaraman (1975). In one case, the impulse response curve is obtained from the distributed model of a chromatographic column with axial diffusion and a linear adsorption isotherm analyzed by Lapidus and Amundson (1952):

$$\mathcal{D}\, \partial^2 C/\partial Z^2 = V\, \partial C/\partial Z + \partial C/\partial t + (1/\beta)\, \partial C_s/\partial t$$
$$C_s = k_1 C + k_2 \qquad (23)$$

where C, C_s are the concentrations of the adsorbate in the liquid and solid, respectively; β is the fractional void volume in the bed, and Z is the spatial coordinate in the axial direction. V and $\mathcal{D}$ are the interstitial velocity of the fluid and the diffusivity of the adsorbate in the fluid, respectively. The boundary conditions for a step change in the inlet concentration are

$$C = C_o, \quad Z = 0, \quad t > 0$$
$$C \text{ finite}, \quad Z \to \infty, \quad t > 0 \qquad (24)$$

The initial conditions are

$$C = C_i \qquad t = 0, \quad Z > 0$$
$$C_s = k_1 C_i + k_2, \quad t = 0, \quad Z > 0 \qquad (25)$$

The step response is then given by the expression

$$F(m) = \frac{C - C_i}{C_o - C_i} = \frac{1}{2}\left[1 + \exp\left(\sqrt{\frac{mV}{4\beta\nu\mathcal{D}}} - Z\sqrt{\frac{\beta\nu V}{4m\mathcal{D}}}\right) + \exp(VZ/\mathcal{D})\,\mathrm{erfc}\left(\sqrt{\frac{mV}{4\beta\nu\mathcal{D}}} + Z\sqrt{\frac{\beta\nu V}{4m\mathcal{D}}}\right)\right] \qquad (26)$$

where $m = V\beta t$, $\nu = 1 + k_1/\beta$. The impulse response is approximated by the response to a narrow pulse of duration $\tilde{t}$:

$$C(Z, t) = C_o\,[F(m) - F(m - V\tilde{t})]$$

where $\tilde{t}$ is sufficiently small. The values chosen for the various parameters are

$$V = \mathcal{D} = 20, \quad \beta = \nu = 5, \quad C_i = 0,$$
$$C_o = 0.1, \quad \tilde{t} = 0.1, \quad Z = 10 \qquad (27)$$

The calculated C must be scaled up by a factor of 100 to obtain the unit impulse response plotted in Figure 5.

The time delay is chosen to be 0.5 and the origin shifted accordingly on the time axis. Three zero Markov parameters are then found adequate. The first nonzero Markov parameter is 51.29. The Markov parameters estimated by the stagewise regression procedure, observing the bounds at each stage, are listed below after normalizing with respect to the first nonzero parameter:

$$0,\ 0,\ 0,\ 1,\ -12.67,\ 106.2,\ -750.25 \qquad (28)$$

Since the intensity function is monotone increasing for this system, the lowest-order partial realization of dimension 4 may be adequate. The zeroth moment is used to obtain the remaining Markov parameter required, Y_7. Here, the zeroth moment $= 51.29/\alpha_4$. The area under the curve is 1. In general, when the zeroth moment is taken into account, the first nonzero Markov parameter is even more important than otherwise, since it also determines the last parameter required. The resulting realization matrices are

$$A = \begin{bmatrix} -12.67 & 1 & 0 & 0 \\ -54.34 & 0 & 1 & 0 \\ -93.32 & 0 & 0 & 1 \\ -51.29 & 0 & 0 & 0 \end{bmatrix}; \quad b = \begin{bmatrix} 0 \\ 0 \\ 0 \\ 1 \end{bmatrix}; \quad c = [51.29 \quad 0 \quad 0 \quad 0] \qquad (29)$$

The original impulse response and the impulse response predicted by the model in (29) are compared in Figure 5. The agreement is fair; except between $t = 1$ and $t = 2$, the error is less than 10%.

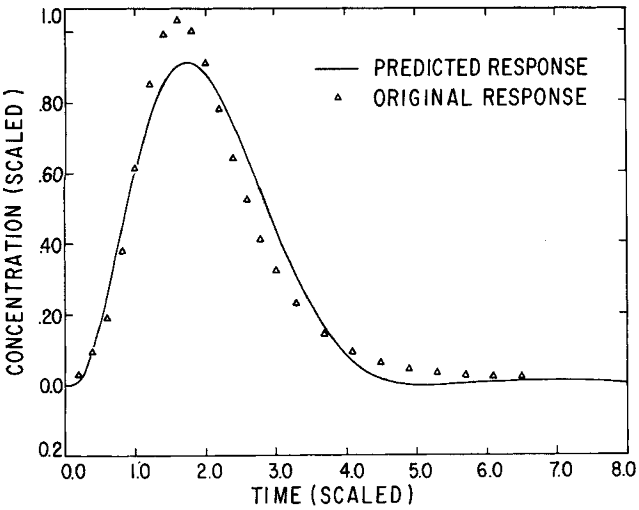

Fig. 7. Pulse response for nonporous packing.

To indicate the sensitivity of the response modes identified to the parameters involved, the impulse response predicted by a modified fourth-order realization with no zeros is compared with the original impulse response in Figure 6. The agreement here is very good; the error is less than 5% throughout. The matrices of the modified realization are

$$A = \begin{bmatrix} -13 & 1 & 0 & 0 \\ -53 & 0 & 1 & 0 \\ -83 & 0 & 0 & 1 \\ -42 & 0 & 0 & 0 \end{bmatrix} ; \quad b = \begin{bmatrix} 0 \\ 0 \\ 0 \\ 1 \end{bmatrix} ;$$

$$c = [42 \quad 0 \quad 0 \quad 0] \qquad (30)$$

THE EMPIRICALLY MEASURED RTD

Finally, let us consider the residence time density function measured by Schiesser (1959) for the liquid phase in trickle flow through a packed bed with nonporous packing. The data used is tabulated in Jayaraman (1975). Choosing a time delay of 12.5 s, and the following scales

$$t = (t' - 12.5)/5$$
$$g = 10\, g' \qquad (31)$$

we obtain three zero Markov parameters and the following set of normalized Markov parameters:

$$0,\ 0,\ 0,\ 1,\ -10.95,\ 94.84,\ -797.58 \qquad (32)$$

The value of the first nonzero Markov parameter obtained is 32.65, and the area under the curve, with the specified scales, is 2. Here, too, the intensity function is monotone increasing. Proceeding along the same lines as in the previous example, we obtain the following fourth-order realization with no zeros:

$$A = \begin{bmatrix} -10.95 & 1 & 0 & 0 \\ -25.01 & 0 & 1 & 0 \\ -33.06 & 0 & 0 & 1 \\ -16.33 & 0 & 0 & 0 \end{bmatrix} ; \quad b = \begin{bmatrix} 0 \\ 0 \\ 0 \\ 1 \end{bmatrix} ;$$

$$c = [32.65 \quad 0 \quad 0 \quad 0] \qquad (33)$$

The impulse response predicted by this model is compared with the original impulse response in Figure 7. Till $t = 1$, the predicted response is extremely close; near the peak, between $t = 1$ and $t = 2$, the error is about 15%; after $t = 2$, there is a closer match between the two curves. This comparison is similar to the match between predicted and original response curves for the previous example of a chromatographic column. Hence, if necessary, it should be possible to modify the realization slightly as before to obtain a better match in the later portions.

This last example illustrates how state variable models may be obtained to use state feedback in real process control situations. A practical limit on the dimension of such state variable models is five. The time scale of interest must be chosen carefully, since time constants of $O(10)$ to $O(1)$ alone may be identified reliably by this procedure. However, as we have already mentioned, the computer time required for processing the relevant pulse response data is extremely small and should pose no problem in updating such low-order linear models with shifts in process characteristics.

ACKNOWLEDGMENT

The authors wish to acknowledge the support of this work from the National Science Foundation Grant GK-42622.

LITERATURE CITED

Ackerman, J. E., and R. S. Bucy, *Information and Control,* **19,** 3, 224 (1971).

Audley, D. R., and D. A. Lee, *IEEE Trans. Auto. Contr. AC-19,* **6,** 738 (1974).

Audley, D. R., and W. J. Rugh, Preprints, Princeton Information Conference, N.J. (1973).

Barlow, R. E., and F. Proschan, *Mathematical Theory of Reliability,* Wiley, New York (1967).

Bassingthwaite, J. B., *Science,* **167,** 1347 (1970).

Beaton, A. E., and J. W. Tukey, *Technometrics,* **16,** 2, 147 (1974).

Beckenbach, E. F., and R. Bellman, *Inequalities,* Springer Verlag, New York (1961).

Bennett, A., and F. Goodridge, *Trans. Inst. Chem. Engrs.,* **48,** T232 (1970).

Bergner, P. E., K. Takeuchi, and Y. Y. Lui, *Math. Biosciences,* **17,** 315 (1973).

Brockett, R. W., *IEEE Trans. Auto Contr. AC-10,* 4, 129 (1965).

Bruni, C., A. Isidori, and A. Ruberti, *IEEE Trans. Auto Contr. AC-14,* 4, 203 (1969).

Feller, W., *An Introduction to Probability Theory and its Applications,* Vol. II, 2 ed., Wiley, New York (1971).

Gantmacher, F. R., *The Theory of Matrices I and II,* Chelsea Publishing Co., New York (1959).

Hearon, J. Z., *Annals Acad. Sci.,* **108,** 36 (1963).

Hirschmann, I. I., and D. V. Widder, *The Convolution Transform,* Princeton Univ. Press, N.J. (1955).

Ho, B. L., and R. E. Kalman, *Regelungstechnik,* **14,** 545 (1966).

Hoerl, A. E., *Chem. Eng. Progr.,* **58,** 3, 54 (1962).

Hoogendorn, C. J., and J. Lips, *Can. J. Chem. Eng.,* **43,** 125 (1965).

Hunt, B. R., *IEEE Trans. Auto. Contr. AC-17,* 703 (1972).

Jayaraman, K., Ph.D. thesis, Princeton Univ., N.J. (1975).

Kalman, R. E., P. L. Falb, and M. A. Arbib, *Topics in Mathematical System Theory,* Chapt. 10, McGraw-Hill, New York (1969).

Kalman, R. E., *SIAM J. Contr.,* **1,** 52 (1963).

———, in *Aspects of Network and System Theory,* R. E. Kalman, and N. Declaris, ed., Holt, Rinehart and Winston, New York (1971).

Karlin, S., *Total Positivity I,* Stanford Univ. Press, Calif. (1968).

———, and J. MacGregor, *J. Math. Anal. Appl.,* **1,** 163 (1960).

Lapidus, Leon, *Ind. Eng. Chem.,* **49,** 1000 (1957).

———, and N. R. Amundson, *J. Phys. Chem.,* **56,** 948 (1952).

Naor, P., and R. Shinnar, *Ind. Eng. Chem. Fundamentals*, 2, 4, 278 (1963).
Rescigno, A., and G. Segre, *Drugs and Tracer Kinetics*, Blaisdell Publishing Co., Mass. (1966).
Rissanen, J., *SIAM J. Contr.*, 9, 3, 420 (1971).
Rossen, R. H., Ph.D. thesis, Princeton Univ., N.J. (1972).
Schiesser, W. E., Ph.D. thesis, Princeton Univ., N.J. (1959).
Sheppard, C. W., *Basic Principles of the Tracer Method*, Wiley, New York (1962).
Silverman, L. M., *IEEE Trans. Auto. Contr. AC-16*, 6, 554 (1971).
Tether, A. J., *IEEE Trans. Auto. Contr. AC-15*, 4, 427 (1970).
van Swaaij, W. P., J. C. Charpentier, and J. Villermaux, *Chem. Eng. Sci.*, 24, 1083 (1969).
Widder, D. V., *The Laplace Transform*, Princeton Univ. Press, N.J. (1946).
Wilkinson, J. H., *The Algebraic Eigenvalue Problem*, Clarendon Press, Oxford (1965).
Willems, J. C., *Archives for Rational Mech.*, 45, 5, 352 (1972).

Manuscript received September 15, 1975; revision received and accepted November 25, 1975.

Fluid and Particle Entrainment Into Vertical Jets in Fluidized Beds

The flow of particles and fluid in the vicinity of vertical jets in fluidized beds was studied by using a two-dimensional bed of lead shot fluidized by water. It was found that both interstitial fluid and solid particles are entrained into the jet as it expands and penetrates into the bed. An approximate mathematical model is developed to describe the particle and fluid flow fields observed experimentally; from this, an expression is derived for rates of entrainment into vertical jets in fluidized beds, and a model is postulated for the flow fields around grid jets.

J. M. D. MERRY

Westinghouse Research Laboratories
Pittsburgh, Pennsylvania 15235

SCOPE

Fluid issuing from the distributor plate at the base of a fluidized bed takes the form of a dilute phase torch or jet which penetrates into the bed of particles. For processes involving chemical reaction, heat transfer, or mass transfer, the mechanism of the jetting region can be extremely important (Behie and Kehoe, 1973; Toei, 1973; Halow, 1974), yet, despite extensive literature on fluidization, little attention has been focused on this region of the bed.

In the multistage fluidized bed coal gasification processes (Lemezis and Archer, 1973), the combustion zone for process heat generation is often a vertical air jet in the lower leg of the combustor/gasifier vessel, into which char fines are fed. This lower leg also acts as the residual ash agglomerator, and the mean particle size there will be considerably larger than the mean size of the injected char fines. It was reasoned that the fines would tend to follow the path of the interstitial fluid rather than that of the larger agglomerates. To discover the likely route of the injected fines and so determine how best to feed fines to the bed so that they would be carried into the combustion jet, an experiment was set up to investigate the flow of interstitial fluid in the vicinity of a vertical jet in an incipiently fluidized bed.

This work has resulted in a better understanding of jet behavior in fluidized beds, and the insight gained has been used in developing a conceptual design for a commercial combustor/gasifier (Merry et al., 1975). A mathematical model of the flow fields around the jet leads to an approximate expression for estimating rates of entrainment of fluid and particles into the jet, and this in turn could lead to improved modeling of the jetting regions of fluidized beds. Application of the model is illustrated by using two examples from the literature.

CONCLUSIONS AND SIGNIFICANCE

An experimental investigation of vertical water jets into a two-dimensional water fluidized bed of lead shot has revealed that interstitial fluid as well as solid particles are entrained into the jet stream as the jet expands and penetrates into the bed. There appears to be a dividing streamline in the fluid such that all the fluid inside this streamline is entrained into the jet, while the fluid outside bypasses the jet and continues to flow upward through the bed. Fine particles or fluid which are to be fed into the jet should be injected inside the dividing streamline in the fluid. The appearance of the jet and the motion of the particles in the liquid-solid system are very similar to the reported observations of Markhevka et al. (1971) and Zenz (1968, 1971) for gas-solid systems, and it is considered that the results presented here will apply equally to either fluid-solid combination.

By representing the effect of the jet on fluid and particle motion in the particulate phase of the bed by a sink, an approximate two-dimensional mathematical model has been developed which describes the solid particle and interstitial fluid flow fields around the jet. This successfully predicts the experimentally observed positions of the dividing streamline in the fluid.

The rate of entrainment of particles and fluid into the jet is directly related to the strength of the sink representing the effect of the jet. By making some simplifying assumptions to the mathematical model, an algebraic expression [Equation (8)] is obtained from which reasonable estimates can be made for the rates of particle and fluid entrainment into two-dimensional and axisymmetric vertical jets in fluidized beds. This expression is

J. M. D. Merry is with the Computer Aided Design Centre, Madingley Road, Cambridge CB3 OHB England.